 doi:10.20944/preprints201906.0167.v1

Article

A Meso-Scale Approach to Estimating Vertical Mixing Induced by Wind–Waves

Vladislav Polnikov[1]*

[1] Obukhov Institute of Atmospheric Physics of RAS, Moscow 119017, Russia; polnikov@mail.ru

* Correspondence: polnikov@mail.ru; Tel.: +7-916-3376728

Abstract: The aim of work is to derive an explicit expression for a function of vertical mixing induced by wind-waves. To this end, in the Navier-Stokes equations, a current is decomposed into four constituents: the mean flow, the wave-orbital motion, the wave-induced turbulent and the background turbulent currents. This decomposition allows separating the wave-induced Reynolds stress, R_w, from the background one, R_b. To make a statistical closure for R_w, the Prandtl approach for the background turbulent fluctuations is used that results in an implicit expression for the wave-induced vertical mixing function, B_v. Expression for B_v is specified based on the author's results for the eddy viscosity found earlier in the frame of the three-layer concept for a wavy air–sea interface, used for modelling wind-drift currents [1]. Finally, the explicit parameterization for $B_v(a, u_*, z)$ is found as a linear function in both the wave amplitude at depth z, $a(z)$, and the friction velocity in the air, u_*. The linear dependence of function $B_v(a)$ on the wave amplitude provides the enhanced vertical mixing induced by wind–waves in comparison with function $B_v(a)$ having the cubic dependence found in [2], as far as the wind-wave amplitude $a(z)$ decays exponentially with depth.

Keywords: air-sea interface; wind–waves; turbulent currents; Reynolds stress; vertical mixing; eddy viscosity

---

1. Introduction

1.1. Three approaches in the problem

An adequate description of the upper-ocean mixing processes is very important for the ocean-circulation modelling from both scientific and practical viewpoints. This was repeatedly mentioned for more than fifty years in numerous papers (e.g., [3-14]). The scientific interest in the problem is determined by the natural aspiration of researchers to clarify the physics of mixing processes in the upper ocean. The practical significance of solving the upper-ocean mixing problem is stipulated by the tasks of improving both the ocean-circulation simulations and forecasting the weather and climate variability. Certain geophysical applications of such solutions are well represented in the recent papers [14-17].

According to the formulations systemized long ego by Mellor and Yamada [18], the traditional approach to the problem is based on using the multi-level schemes for statistical moments of hydrodynamic variables. This approach is based on the full Navier-Stokes equations describing motions of different scales of variability that leads to a necessity to derive a set of evolution equations for statistical moments of different variables. On this way, an evident progress was achieved (e.g., [6, 14, 15, 19, 20]). However, the mentioned approach contains numerous physical assumptions, hypotheses and simplifications. Eventually, all these uncertainties result in

Preprints (www.preprints.org) | NOT PEER-REVIEWED | Posted: 18 June 2019 doi:10.20944/preprints201906.0167.v1

underestimation of a vertical mixing in the upper layer and a mixed-layer depth (see citations in [2, 13, 15] among others).

The approach based on the full Navier–Stokes equations is usually applied to consideration of the global circulation that corresponds to the large-scale description of ocean motions. In this approach they take into account the Earth's rotation and the Stokes drift. The instability of the latter, enforced by surface waves and a wind stress, results in an appearance of the large-scale mixing process in the upper layer, which is referred to as the Langmuir turbulence [14, 21-23]. This type of turbulence has the scale corresponding to the ocean-boundary layer with the size of about hundred meters [14]. Studying of this phenomenon provided a radical progress in understating the role of the large-scale turbulence mixing in the global circulation (e.g., [11, 14, 20] among others). Herewith, the meso-scale orbital motions of wind waves are not directly taken into consideration in this large-scale approach.

Nowadays it seems that an additional progress in solving the problems of the upper-layer dynamics could be obtained if one takes into account another type of mixing provided by the meso-scale turbulent process. This kind of mixing is described by local features of direct interaction between the meso-scale orbital wind-wave motions and the background large-scale ones. In this approach, hereafter referred to as *the local wave-current interaction approach* (shortly, local approach), the Earth's rotation is omitted, and the Stokes drift is considered as a negligible flow [2, 5].

The local approach in the mixing problem is based on the concept of the meso-scale wave-induced turbulence which is considered as an addition to the large-scale background turbulence. Existence of the former type of turbulence was justified and confirmed in numerous experimental and theoretical studies (see [24-26] and references therein). In particular, Babanin [25] defined the local Reynolds number, *Re*, provided by the orbital wave motions, as: $Re \equiv a^2\omega_p / \nu_w$, and found that the wave-induced turbulence below a surface emerges when *Re* becomes greater of 10^3. Here, a is the mean wave-amplitude, ω_p is the dominant wave frequency, and ν is the kinematic viscosity of water. This gives an estimate that the meso-scale wave-induced turbulence may origin if a wave height exceeds several centimeters. Consequently, the meso-scale wave-induced turbulence should be widely spread. This conclusion was confirmed in the laboratory experiments with non-breaking waves [27, 28], and in the field measurements dealing with breaking waves (e.g., [29, 30]).

Intensity of a turbulence mixing is measured by the dissipation rate of the turbulent kinetic energy (DRT), ε [5, 19, 24, 27, 29, 31]. For non-breaking waves, the direct measurements in a tank [27] provided estimate of ε of the order of 10^{-3} m^2s^{-3} and showed the cubical dependence of ε on wave amplitude a. In the case with breaking waves, intensity of the wave-induce turbulence is of several orders greater [29, 30]. Though, such intensive wave-induced turbulence is mainly located in the vicinity of a wavy surface, which has the size of about a wave height. For this reason, the wave-breaking turbulence provides a special type of vertical mixing which can be referred to as the small-scale one. In our mind, this kind of the wave-induced mixing needs a separate consideration.

Really, the size of the layer with an intensive wave-breaking (breaking layer) is of the order of a mean wave height [5, 19, 29, 30]. More precisely, it is of the order of several meters at most [32]. In turn, the meso-scale turbulence is spread through the depth of about a half of length for dominant surface wave [12], i.e., it is in an order greater than the width of the breaking layer (retaining much smaller than the depth of the Langmuir turbulence due to an order greater scale of the wave-orbital velocity with respect to the Stokes drift). Such a significant difference in the spatial scales allows considering the discussed turbulent processes separately.

Thus, one may state that the meso-scale turbulence, described by the local approach determined above, is the main wave-current interaction process which takes place in the upper layer between the deepest wave troughs and the depth about a half of dominant wave length (see [25, 29, 31] and references therein). In this range of depths, referred to as the water-boundary layer, the wave breaking processes could be implicitly accounted as one of the reasons providing appearance of the local wave-induced turbulence, for example, due to production of an additional vertical momentum

Preprints (www.preprints.org) | NOT PEER-REVIEWED | Posted: 18 June 2019 doi:10.20944/preprints201906.0167.v1

flux [2, 15]. This discrimination of the breaking processes could be considered as an additional circumstance for applicability of the local approach in the problem of wave-induced mixing.

For the first time the local approach defined above was successfully applied in [2] to solve the problem of the wave-induced vertical mixing. These authors derived an analytical expression for the vertical-mixing function, B_v, and applied it as an addition to the traditional turbulent mixing coefficients in the ocean-circulation model POM. Finally, they found numerically that the meso-scale turbulence processes, induced by surface waves, can reasonably enhance the large-scale mixing in the upper ocean, providing a better correspondence between simulations and observations for the depth of the mixing layer [2]. Later, the similar results of the local approach applications were confirmed in [13].

Thus, the local approach turned out to be rather effective in solving the problem of the wave-induced vertical mixing. However, this approach could be updated by a further elaboration. To clarify this statement, let us dwell on the derivations made in [2].

1.2. The local approach version used in [2]

Qiao et al. [2] started their derivation for the wave-induced mixing function directly from the statistical closure of the Reynolds stress, $<u_i u_j>$, appearing after averaging the motion equations over the wave scales (hereafter, brackets $<\ldots>$ mean the wave-ensemble averaging). In the mentioned Reynolds stress, they decomposed the total current fluctuation, u_i, into the wave-induced one, $\tilde{u}_i'$, and the turbulent fluctuation existing without waves, u_i'. This allows to extract the sought wave-current interaction stress, $<\tilde{u}_i' u_j'>$, which was expressed via wave parameters.

In the simplest case of the one-dimensional shear mean current, $\bar{\mathbf{U}} = (U(z),0,0)$, for the certain vertical mixing stress, $<\tilde{u}_3' u_1'> + <\tilde{u}_1' u_3'>$, they assumed the following statistical closure:

$$-(<\tilde{u}_3' u_1'> + <\tilde{u}_1' u_3'>) = B_v \frac{dU}{dz}. \tag{1}$$

Hereafter, sub-indexes 1,2,3 denote the x-, y-, z- components of currents, and factor B_v is defined as the wave-induced vertical eddy (turbulent) viscosity (diffusivity), considered as the vertical-mixing function. Qiao et al. [2] specified the expression for B_v in the form

$$B_v = <\tilde{\lambda}_3' \tilde{u}_3'> \quad , \tag{2}$$

where $\tilde{\lambda}_3'$ is the mixing length of the wave-induced turbulence.

To clarify the derivation of Eq. (2), we note that Eq. (1) means applying the Prandtl approximation for the background fluctuation, u_i', in the form

$$u_i' = \lambda_i' (dU(z)/dz) \qquad (I = 1,3) \quad , \tag{3}$$

where λ_i' is the stochastic mixing length for the background turbulence. Then, λ_i' was replaced (arbitrary) by the mixing length for the wave-induced turbulence, $\tilde{\lambda}_3'$, what results in Eq.(2).

Preprints (www.preprints.org) | NOT PEER-REVIEWED | Posted: 18 June 2019 doi:10.20944/preprints201906.0167.v1

Farther, Qiao et al. [2] expressed the wave-induced fluctuation, $\tilde{u}_3'$, via the wave-number spectrum of waves at a surface, $S(\mathbf{k})$, in the form (at depth *z*; the z-axes is directed upward)

$$\tilde{u}_3'(z) = \tilde{\lambda}_3'(z) \cdot \frac{d\left(\int \omega^2(\mathbf{k}) S(\mathbf{k}) exp(2kz) d\mathbf{k}\right)^{1/2}}{dz} , \tag{4}$$

what, in essence, is the form of the Prandtl approximation applied to $\tilde{u}_3'$. Thus, they wrote:

$$B_v(z) = <\tilde{\lambda}_3'(z)\tilde{u}_3'(z)> = <\tilde{\lambda}_3'^2(z)> \cdot \frac{d\left(\int \omega^2(\mathbf{k}) S(\mathbf{k}) \exp(2kz) d\mathbf{k}\right)^{1/2}}{dz} . \tag{5}$$

To specify the expression for $B_v(z)$, Qiao et al.[2] proposed that $<\tilde{\lambda}_3'^2(z)>$ can be expressed via the mean amplitude of the orbital wave motions at depth *z*, $<a(z)>$. The final expression for the wave-induced mixing function, B_v, gets the form (for more details see the original paper)

$$B_v(S,z) = \alpha \int S(\mathbf{k}) \exp(2kz) d\mathbf{k} \cdot \frac{d\left(\int \omega^2(\mathbf{k}) S(\mathbf{k}) \exp(2kz) d\mathbf{k}\right)^{1/2}}{dz} . \tag{6}$$

The first factor in the r.h.s. of (6) corresponds to the second power of the mean mixing length, $<(\tilde{\lambda}_3')^2>$, the second one to the vertical gradient of the averaged wave orbital velocity. In Eq. (6), α is the dimensionless fitting coefficient, $\omega(\mathbf{k})$ is the wave frequency corresponding to wave vector $\mathbf{k}$ for gravity waves, and the exponents denote the depth dependence for the surface wave spectrum.

Besides the exponential decay with depth, the main feature of Eq. (6) is the cubic dependence of function $B_v(S,z)$ on the mean wave amplitude, $<a(z)>$. Due to the exponential decay for a wave amplitude, $<a(z)> = a(0)\exp(kz)$, Eq. (6) results in the ratio

$$B_v(S,z) \propto <a(z)>^3 \propto \exp(3k_p z) ,$$

where k_p is the wave number corresponding to the peak of spectrum**.** Despite of this circumstance, Qiao et al. [2] stated: "… *adding B_v to the vertical diffusivity in a global ocean-circulation model yields a temperature structure in the upper 100 m that is closer to the observed climatology than in a model without the wave-induced mixing*" (the citation from [2]). Later, the fact of remarkable impact of the proposed wave-induced mixing on the global circulation was confirmed in the series of works (e.g., [13, 16]).

Referring to the said, it seems that the presented approach is as a very prospective semi-phenomenological solution of the wave-induced mixing problem. Though, this approach is worthwhile to be elaborated with the aim of improving some weak theoretical points in the Qiao's version, namely: (i) the replacing λ_1' by $\tilde{\lambda}_3'$ in Eq. (2), and (ii) the closure in Eq. (5). Besides, it needs

 doi:10.20944/preprints201906.0167.v1

to provide all details of the derivation of the form for the initial Reynolds stress considered in [2], what is necessary for understanding a range of the approach applicability.

The present paper is aimed to develop a new version of the Qiao's approach with the proper theoretical justification for it. Eventually, it turned out that the new version results in a reasonably greater impact of waves on the vertical mixing than it is described by Eq. (6).

2. Main derivations

2.1. Theoretical background

With the aim of representing important details in the convincing form and to introduce details of the problem, here we reproduce some known analytical derivations. Herewith, one should keep in mind that we deal with the motions in the upper water layer located below the deepest troughs of wavy surface: from $z < -2a(0)$ down to the depth of about a wave length of the dominant surface wave. In the frame of the local approximation, the considered scales correspond to the averaging over several tens of the dominant wave period and the proper length. For generality, we suppose that a certain background turbulent current exists in the upper layer independently of the surface waves.

Following to the traditional theoretical derivations [19, 31], we start from the Navier–Stokes equations written in the tensor form:

$$\frac{\partial U_i}{\partial t} + U_j \frac{\partial U_i}{\partial x_j} = -\frac{1}{\rho_w}\frac{\partial P}{\partial x_i} + \nu \frac{\partial^2 U_i}{\partial x_j^2} \quad . \tag{7}$$

Here U_i (i=1,2,3) is the x-y-z-component of the current, P is the pressure, ρ_w is the water density, and ν is the kinematic viscosity of the water. (Repeating indexes mean the summation). Note that in the local approach for this task (see Sec. 1a), the Coriolis term is not included in (7).

Before making statistical averaging, it is very important to separate accurately different kinds of motions. To this end, we put the following decomposition for the current:

$$U_i = \hat{U}_i + u_i = (\bar{U}_i + \tilde{U}\delta_{i,1}) + \tilde{u}_i + \tilde{u}_i' + u_i' \quad . \tag{8}$$

Here $\hat{U}_i \equiv \bar{U}_i + \tilde{U}_d \delta_{i,1}$ is the mean current which includes the background flow, $\bar{U}_i$ (existing without waves), and the drift current, $\tilde{U}_d \delta_{i,1}$, provided by both the wind and the waves [33] and directed along the OX axes (denoted by symbol $\delta_{i,1}$); u_i is the total turbulent addition to mean

 doi:10.20944/preprints201906.0167.v1

current $\hat{U}_i$.[1] In our case, the summand u_i includes the following set of terms: the wave orbital velocity, $\tilde{u}_i$, the wave-induced turbulent fluctuation, $\tilde{u}_i'$, and the turbulent fluctuation existing in the absence of waves, u_i'. Hereafter, summand u_i' is referred to as the "background" turbulence.

Note the following: (i) the orbital velocity $\tilde{u}_i$ does not belong to the turbulent motions; (ii) the background turbulent fluctuation, u_i', is independent of the turbulent motions induced by waves, $\tilde{u}_i'$; (iii) both fluctuations, u_i' and $\tilde{u}_i'$, may correlate statistically with each other. The latter item is the assumption which is very important for the following consideration.

A similar decomposition is assumed for pressure P (without the drift terms). But below we shall not touch the pressure terms in Eq. (7), supposing that, in this version of our constructions, they do not significantly effect on the wave-induced vertical mixing under consideration, being responsible mainly for the turbulent energy and the momentum flux production in the narrow breaking layer [15,19].

To arrive to the Reynolds stress considered in [2] (i.e., the l.h.s. of Eq. 1), the following statistical approximations should be accepted:

1) All the additional summands in Eq. (8) vanish in the mean:

$$<\tilde{u}_i>=0;\ <\tilde{u}_i'>=0;\ <u_i'>=0 \qquad \text{(i.e., } <U_i>=\hat{U}_i\text{).} \tag{9a}$$

2) There is no correlation between the mean, the wave orbital and the turbulent motions:

$$<\hat{U}_i\tilde{u}_j>\ =0;\ <\hat{U}_i\tilde{u}_j'>=0;\ <\hat{U}_i u_j'>=0. \tag{9b}$$

The same is true for the wave orbital velocities and the turbulent fluctuations:

$$<\tilde{u}_i\tilde{u}_j'>=0;\ <\tilde{u}_i u_j'>=0. \tag{9c}$$

Formally, Eqs. (9b, c) correspond to the assumption of no correlation between motions of different scales, what is typical for the turbulence theory [16, 31].

3) The wave-induced and the background-turbulent summands may correlate:

$$<\tilde{u}_i'\tilde{u}_j'>\neq 0;\ <\tilde{u}_i'u_j'>\neq 0;\ \text{ and }\ <u_i'u_j'>\neq 0. \tag{9d}$$

Additionally, the condition of continuity takes place for each constituent in (8): $\partial U_i/\partial x_i = 0$.

Substituting (8) into (7), making the ensemble averaging, and taking into account ratios (9a, b), one obtains the Reynolds equations,

---

[1] Formally, the Stokes drift is included into the total drift-current term, $\tilde{U}\delta_{i,1}$, though due to its smallness with respect to wind drift (according to [33], the Stokes drift is less than 15% of the wind drift), this term is not so important here. Besides, the case of no wind is out of our consideration.

Preprints (www.preprints.org) | NOT PEER-REVIEWED | Posted: 18 June 2019 doi:10.20944/preprints201906.0167.v1

$$\frac{\partial \hat{U}_i}{\partial t}+\hat{U}_i\frac{\partial \hat{U}_i}{\partial x_j}+\frac{\partial < u_j u_i >}{\partial x_j}=\left[pressure-terms\right]+\nu\frac{\partial^2 \hat{U}_i}{\partial x_j^2}, \tag{10}$$

where the third term in the l.h.s. contains Reynolds stress $< u_j u_i >$. In view of the above decomposition, full expression for the stress is,

$$\begin{aligned} &< u_j u_i > = < \tilde{u}_j \tilde{u}_i > + < \tilde{u}_j \tilde{u}_i' > + < \tilde{u}_j u_i' > + \\ &+ < \tilde{u}_j' \tilde{u}_i > + < \tilde{u}_j' \tilde{u}_i' > + < \tilde{u}_j' u_i' > + < u_j' \tilde{u}_i > + < u_j' \tilde{u}_i' > + < u_j' u_i' > \end{aligned} . \tag{11}$$

Using ratios (9c, d), from (11) one may find,

$$< u_j u_i > = < \tilde{u}_j \tilde{u}_i > + < \tilde{u}_j' \tilde{u}_i' > + < \tilde{u}_j' u_i' > + < u_j' \tilde{u}_i' > + < u_j' u_i' > . \tag{12}$$

If there are no waves, i.e., when $\tilde{u}_i = 0$, and $\tilde{u}_i' = 0$, one finds the standard Reynolds stress

$$< u_j u_i > = < u_j' u_i' > \tag{13}$$

corresponding to the background turbulence existing with no waves.

In the case of no waves, the first-level closure approximation [31] gives:

$$- < u_j' u_i' > = K_{ji} \partial \bar{U}_i / \partial x_j , \tag{14}$$

where coefficient K_{ji} has the meaning of the eddy (turbulent) viscosity (at the depth considered). For constant value of K_{ji}, closure (14) leads to the standard form of the viscous term in Eq. (7),

$$-\frac{\partial < u_j' u_i' >}{\partial x_j} = \frac{\partial}{\partial x_j}\left(K_{ji}\frac{\partial \bar{U}_i}{\partial x_j}\right) = K_{ji}\frac{\partial^2 \bar{U}_i}{\partial x_j^2} . \tag{15}$$

By this way, making the closure of the wave-induced terms in stress (12), one may find the wave-induced part of the eddy viscosity corresponding to the vertical-mixing function.

2.2. Initial specifications

For simplicity, let us consider the case of uniform mean current $\hat{\mathbf{U}}$ (including drift $\tilde{U}_d$) with the vertical shear, directed along the OX-axis, i.e.: $\hat{\mathbf{U}}=(U(z),0,0)$. For components $j = 1$ and $i = 3$, Eq. (12) provides the stress under consideration:

$$< u_1 u_3 > = < \tilde{u}_1 \tilde{u}_3 > + < \tilde{u}_1' \tilde{u}_3' > + < \tilde{u}_1' u_3' > + < u_1' \tilde{u}_3' > + < u_1' u_3' > . \tag{16}$$

The stress given by Eq. (16) is to be specified.

First, we consider the case of potential wave-orbital motions and the linear approximation for deep water. In this case, the two-dimensional monochromatic wave with amplitude *a*, frequency *ω*, and wave number *k* is described by the following ratios [34]: the surface elevation is given by

$$\eta(x,t) = a\cos(kx-\omega t); \qquad 17a)$$

the velocity potential is

$$\phi(x,z,t) = a\frac{\omega}{k}\exp(kz)\sin(kx-\omega t); \tag{17b}$$

 doi:10.20944/preprints201906.0167.v1

the orbital velocities are

$$\tilde{u}_1 = u_x = a\omega exp(kz)cos(kx-\omega t) \quad \text{and} \quad \tilde{u}_3 = u_z = a\omega exp(kz)sin(kx-\omega t). \tag{17c}$$

Second, using ratios (17c), due to the orthogonality of oscillating functions $\tilde{u}_1$ and $\tilde{u}_3$, one may find that

$$<\tilde{u}_1\tilde{u}_3> \ = 0. \tag{18}$$

To estimate $<\tilde{u}_1^{'}\tilde{u}_3^{'}>$, we use the Prandtl approximation for the wave-induced turbulent motions in the form

$$\tilde{u}_i^{'} = \tilde{\lambda}_i^{'}\partial\tilde{u}_i / \partial x_3 \tag{19}$$

($i = 1, 3$). Then, using of Eqs. (17c) and Eq. (19) yields,

$$<\tilde{u}_1^{'}\tilde{u}_3^{'}>=<\lambda_1^{'}\lambda_3^{'}>\cdot<(\partial\tilde{u}_1/\partial x_3)(\partial\tilde{u}_3/\partial x_3)> \ = \ <\tilde{\lambda}_1^{'}\tilde{\lambda}_3^{'}>\cdot k^2\cdot<\tilde{u}_1\tilde{u}_3>=0, \tag{20}$$

for the same reason as in Eq. (18).

Note that Eq. (20) does not contradict to the first equality in Eq. (9c): $<\tilde{u}_i\tilde{u}_j^{'}> = 0$, as far as the substitution of Eq. (19) into Eq. (9c) yields

$$<\tilde{u}_i\tilde{u}_j^{'}>=<\tilde{\lambda}_j^{'}>\cdot k\cdot<\tilde{u}_i\tilde{u}_j>=0. \tag{20a}$$

In any case, the zero value for term $<\tilde{u}_i\tilde{u}_j^{'}>$ (Eq. 20) is true due to the random feature of mixing length $\tilde{\lambda}_j^{'}$ for which the equality $<\tilde{\lambda}_j^{'}>= 0$ is true by the definition. (In the case of term $<\tilde{u}_1\tilde{u}_3>$, validity of Eq. (20a) is also provided by the orthogonality for the components used).

Third, excluding the last (background) term in Eq. (16) and using Eqs. (18), (20) yield the following wave-induced stress

$$<u_1u_3>_w=<\tilde{u}_1^{'}u_3^{'}>+<u_1^{'}\tilde{u}_3^{'}> \quad . \tag{21}$$

Due to the spatial homogeneity of the wave-induced turbulence, one may put that the both summands in (21) have the same value (the Prandtl approximation supports this). Thus,

$$<u_1u_3>_w\cong 2<\tilde{u}_1^{'}u_3^{'}> \quad . \tag{22}$$

It is the wave-induced stress, $<u_1u_3>_w$, that provides the addition to the background eddy viscosity. For the first time, Eq. (21) was "*a priory*" postulated and analyzed in [2] (see Sect. 1b). All the assumptions, accepted in this subsection, determine the range of applicability for the results found in [2] and in the following derivations.

2.3. New closure

New approach for the closure of stress (22) has the following steps.

1) The background turbulence fluctuation is expressed by the Prandtl approximation, $u_3' = \lambda_3' \partial \bar{U} / \partial x_3$. Remind here that λ_3' is the unknown random mixing length that has no relation to the wave motions, because fluctuation u_3' (and consequently λ_3') describes the background turbulence. In such a case, the main expression for the farther analysis is as,

$$-< u_1 u_3 >_w \cong 2 < \tilde{u}_1' \lambda_3' > \partial \bar{U} / \partial x_3 . \qquad (23)$$

2) By analogy with Eq. (14), from (23) it follows the implicit expression for the wave-induced eddy viscosity, B_v (with the notation used in [2]), in the form

$$B_v = 2 < \tilde{u}_1' \lambda_3' > . \qquad (24)$$

Thus, it needs to find the closure for statistically averaged value $< \tilde{u}_1' \lambda_3' >$. Note that Eq. (24) for B_v differs from Eq. (2) postulated in [2]. In our case, the background-turbulence mixing length, λ_3', is saved because it cannot be expressed via any part of the wave motions, as we have already mentioned from the very beginning of this subsection.

3) The following features for function $B_v = 2 < \tilde{u}_1' \lambda_3' >$ are stated:

(i) B_v is the statistical moment, the final value of which can be postulated under some assumption, as it is usually used in the theory of turbulence [31];

(ii) $B_v(\tilde{u}_1')$ is the linear function in the wave-induced turbulent fluctuation, $\tilde{u}_1'$. From the physical point of view, one may expect that the dependence $B_v(a)$ (at any depth z) should also be the linear function in the local mean wave-amplitude, $a(z)$, depending on z.

(iii) Turbulent features of the background currents (stochastic features of λ_3') might be related to some already known stochastic processes in the upper layer (not directly depending on the wave motions).

4) To realize the features of B_v stated above, we propose to estimate the statistical moment $< \tilde{u}_1' \lambda_3' >$ on the basis of recent theory for the wind-induced drift currents, constructed in [1]. The main points of this estimation are as follows.

First, we state that the wavy air–sea interface may be conventionally partitioned into three constituents. They are: the air boundary layer (ABL), the wave zone (WZ), and the water boundary layer (WBL). This statement is based on the data processing made in [35] for the numerical results found in [36]. Such a partition was empirically confirmed in the tank observations by Longo et al. [37] as shown in Figure 1.

The meso-scale ABL and WBL have sizes about a wave length of the dominant surface wind-waves. Herewith, the size of the WZ is about of 2-3 mean wave heights [35], i.e., much smaller than that of the ABL and the WBL. The empirical evidence of this fact is given in Figure 1.

Preprints (www.preprints.org) | NOT PEER-REVIEWED | Posted: 18 June 2019 doi:10.20944/preprints201906.0167.v1

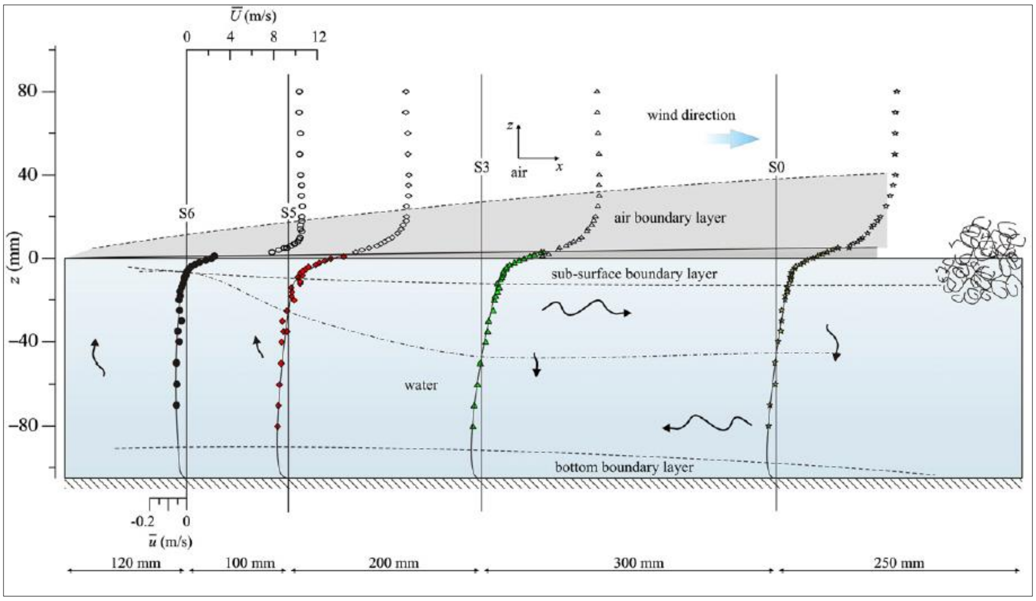

Figure 1. The general scheme for the mean-flow distribution in the interface system (from [37]). The wave zone is evidently seen between the air boundary layer and the (sub-surface) water boundary layer.

The most important feature of this tree-layer structure of the interface is that the vertical profile of the total mean current, $\hat{U}(z)$, is linear in z in the WZ. This fact is directly supported experimentally in [37, 38]. The empirical evidence of this feature is given in Figure 2.

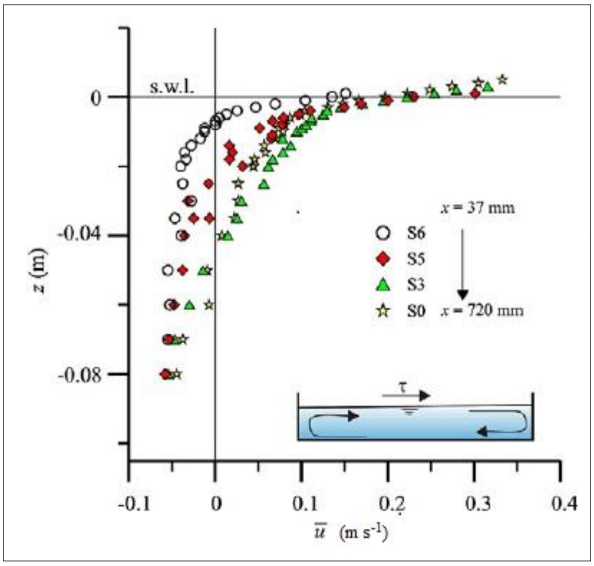

Figure 2. The measured mean current profiles $\overline{u}(z)$ at different points in the tank (from [38]).

Due to the linear profile for a mean current in the turbulent WZ, it is evidently to assume that the WZ has a meaning of the turbulent viscous layer (located between the ABL and WBL), as it is known from the classical turbulent theory [31]. Thus, from the point of view of statistical hydrodynamics, the following conditions should take place in the WZ:

(i) The wind-induced momentum flux, τ_w, directed downward, is constant.

(ii) The eddy viscosity coefficient, K, supporting the linear current profile, $\bar{U}(z)$, is constant.

Thus, the momentum flux balance in the WZ could be written in the form [31]:

$$\tau_w = K \;\partial \bar{U}(z)\,\partial , \tag{25}$$

 doi:10.20944/preprints201906.0167.v1

where K is the eddy viscosity taking place in the WZ. Based on Eq. (25), Polnikov [1] has found that the viscosity coefficient K can be expressed as

$$K = C_K\, u_* a_0 \ , \tag{26}$$

where C_K is the dimensionless coefficient of the order of 10^{-2}, and u_* is the friction velocity in the ABL (for details, see [1]). Equation (26) means that the wave-induced turbulent viscosity coefficient K in the WZ is the linear function in wave amplitude a, what corresponds to the expected dependence for wave-induced mixing function $B_v(a)$ (see item 3(ii) above). This correspondence provides the further derivation.

5) The facts mentioned in item 4) allow us to propose that the sought turbulent viscosity in the WBL, B_v, is the spatial extension for the eddy viscosity coefficient K taking place in the WZ, if we assume the similar physical features for the turbulence in the WZ and WBL. Based on this phenomenological assumption, one may state that, at arbitrary depth z in the WBL, the following equality is true (hereafter the sign " ≈ " means "approximately equal"):

$$B_v(z) \approx K(z), \tag{27}$$

where $K(z)$ is the analytical continuation for function K given by Eq. (26), extended down to depth z in the WBL.

The proposed analytical continuation could be realized via the well-known exponential depth-dependence of a wave amplitude for each spectral component: $a(k,z)=a_0\exp(kz)$, where a_0 is the wave amplitude at a mean water level [12]. Thus, in the case of monochromatic wave on the surface, the explicit depth-dependent expression for $B_v(z)$ obtains the form

$$B_v(z) \approx K(z) \approx c_v \cdot u_* a_0 \exp(kz) \ , \tag{28}$$

where c_v is the dimensionless fitting coefficient of the order of 10^{-2}. Generalization of Eq. (28) for a spectrum of surface waves is given by the equation

$$B_v(z) = c_{Bv} \cdot u_* \left(\int S(\mathbf{k}) \exp(2kz) d\mathbf{k} \right)^{1/2} , \tag{29}$$

where c_{Bv} is the fitting coefficient of the order of 10^{-2}, similar to c_v in Eq. (28).

2.4. Final remarks

Equations (28, 29) finalize the derivation of the sought wave-induced vertical mixing function, B_v. As seen, the principal difference between Eq. (29) and result (6) by Qiao et al. [2] is the linear dependence of the mixing function B_v on the local wave amplitude in Eq. (29): $B_v(z, a) \sim a(z)$. This result leads to a reasonably enhanced intensity for the wave-induced vertical mixing at any fixed depth z in the WBL with respect to the cubic dependence B_v on wave amplitude in (6) due to the radical difference between the exponents in Eqs. (29) and (6).

The dependences $B_v(a_0)$ and $B_v(u_*)$ predicted by Eq. (29) can be verified in future by means of both the numerical simulations alike [39, 40] and the laboratory experiments alike [27, 28]. A

Preprints (www.preprints.org) | NOT PEER-REVIEWED | Posted: 18 June 2019 doi:10.20944/preprints201906.0167.v1

successful verification of these dependences would justify the preference of new version of the model for the wave-induced mixing processes with respect to the known one and vice versa. Some ideas of analytical verification dependences $B_v(a_0)$ and $B_v(u_*)$ are discussed below.

3. Discussion

Let us check the correspondence of result (28) to some known empirical dependences. As far as empirical data of a direct measuring eddy viscosity coefficient B_v (if any) are not known to us, we need to choose proper empirical values relevant to a checking dependences $B_v(a_0)$ and $B_v(u_*)$. The most convenient of them is the dissipation rate of the turbulent kinetic energy (DRT), ε, which is routinely measured in experiments (e.g., [19, 27, 29] among others). To our aim we may use the relation between the wave-induced part of the DRT, ε_w, and the corresponding eddy viscosity, B_v, written in the form [34] [2]

$$\varepsilon_w \sim B_v \left(\partial \tilde{u}_1 / \partial x_3\right)^2 \quad . \tag{30}$$

Equation (30) allows an analytical checking the correspondence of Eqs. (28, 29) to the known dependences of ε_w on surface wave amplitude a_0 and friction velocity u_*.

According to the measurements [27], the following dependence $\varepsilon_w(a_0)$ takes place at any depth in the WBL,

$$\varepsilon_w \propto a_0^3 \quad . \tag{31}$$

The correspondence between ratios (30) and (31) becomes evident, if one takes into account that wave velocity $\tilde{u}_1$ in (30) is linear in wave amplitude a_0 (see Eq. 17c). Thus, the analytical checking dependence $B_v(a_0)$ is successful.

The known dependence of ε_w on u_* in WBL has the kind (e.g., [5, 19, 29],

$$\varepsilon_w \propto u_*^3 \quad . \tag{32}$$

Substituting (28) and (17c) in Eq. (30) yields

$$\varepsilon_w \propto u_* a(\omega_p k_p a)^2 \propto u_* \omega_p^6 \quad , \tag{33}$$

where the transition from k_p to the peak frequency of wave spectrum, ω_p, is made by using the dispersion relation $\omega^2 = gk$ (hereafter, the zero-subindex at wave amplitude a is omitted for

[2] Here, in the r.h.s. of (30), the vertical gradient of the wave-orbital velocity is used as the approximation for getting qualitative estimations. In more general case, the derivative in the r.h.s. of (30) could include the drift current as well.

simplicity). To extract dependence $\varepsilon(u_*)$ from Eq. (33) (in the first guess), one may use the well-known wave-growth empirical dependences for the dimensionless wave energy, $\tilde{E}$, and the peak frequency, $\tilde{\omega}_p$, on the dimensionless fetch, $\tilde{X}$, in the fetch-limited case. They are as follows [32]

$$\tilde{E} \equiv \frac{a^2 g}{u_*^4} \propto \tilde{X} \equiv \frac{Xg}{u_*^2} \qquad \text{and} \qquad \tilde{\omega}_p \equiv \frac{\omega_p u_*}{g} \propto \tilde{X}^{-1/3} \equiv \left(\frac{Xg}{u_*^2}\right)^{-1/3}, \tag{34}$$

where X is the dimensional fetch. From the first part of Eqs. (34), one finds that wave amplitude has the following dependence: $a(u_*) \propto u_*$. From the second part of Eqs. (34), it follows that $\omega_p(u_*) \propto (u_*)^{-1/3}$. Finally, Eq. (33) gets the form

$$\varepsilon_w \propto u_* \omega_p^6 a^3 \propto u_*, \tag{35}$$

what corresponds reasonably to the empirical dependence in Eq. (32), if one take into account inevitable empirical errors in estimates for the power in Eq. (32) and the powers for $\tilde{X}$ in Eqs. (34). Besides, one has to take into account a deviation from the fetch-limited case *in situ* [32].

Thus, the encouraging results of analytical checking the correspondence of Eq. (28) to known empirical dependences (31) and (32) do open a way to its experimental verification. The latter could be realized by estimating empirical dependences $B_v(a_0)$ and $B_v(u_*)$ in the tank experiments similar to ones described in [27, 28].

In addition to the said, it is worthwhile to mention the following. In our mind, the experimental verification dependences $B_v(a_0)$ and $B_v(u_*)$ can be executed by two ways. The first, indirect way could be based on a direct measuring the DRT dependencies, $\varepsilon_w(a_0)$ *and* $\varepsilon_w(u_*)$ in a wind-wave tank, followed by the using the r.h.s. of Eq. (33) for the final comparison of this theory with the experiment. The second, direct way could be realized by means of the estimating the wave-induced vertical mixing function B_v via measuring the rate for a spatial spreading of a small color ink-drop in the water layer below the deepest wave troughs. To this aim, one can use the Einstein's formula: $B_v \sim \langle \Delta z(t) \rangle^2 / \Delta t$ (where $\Delta z(t)$ is the size of a spread ink-drop at time t, and Δt is the time of the drop spreading), keeping in mind the physical similarity between B_v and the diffusion coefficient for the passive particles in a fluid [31]. The proper technique needs its own specification, though it could be easily elaborated when needed.

5. Conclusions

The model for a vertical turbulent-mixing function is derived, which predicts the enhanced impact of the wind-wave motions on the mixing in the water boundary layer located below deepest wave troughs till the depth about a dominant wave length. The model is based on the following three grounds.

Preprints (www.preprints.org) | NOT PEER-REVIEWED | Posted: 18 June 2019 doi:10.20944/preprints201906.0167.v1

First, in the Navier–Stokes equations, the total current is decomposed into the four constituents, including the mean current, the wave-orbital motions, the wave-induced turbulent and the background turbulent currents (Eq. 8). This allows separating the wave-induced Reynolds stress, R_w, from the background one, R_b (Eq. 12).

Second, to close wave-induced stress R_w, the Prandtl approximation for the background turbulence fluctuation is used, resulting in the implicit expression for the wave-induced vertical mixing coefficient, B_v , valid in the water boundary layer (Eq. 24).

Third, the expression for B_v is specified, based on the author's results for the eddy viscosity, K, taking place in the wave zone located between the air and water boundary layers of the air-sea interface (see item 4 in Sect. 2c and Figure 1).The sought eddy viscosity in the upper water layer, B_v , is proposed to be the analytical continuation of the viscosity function describing the analytical dependence of K on a wave amplitude (Eqs. 26, 27). Eventually, the sought mixing function, $B_v(a, z$, u_*), is found to be linear in both depth-dependent wave amplitude $a(z)$ and friction velocity u_* in the air (Eq. 28). Generalization of Eq. (28) for a spectrum of surface waves is given by Eq. (29).

The found result for function $B_v(a)$ means the enhanced impact of waves on the wave-induced vertical mixing with respect to the known cubic dependence of $B_v(a)$ described by Eq. (6) presented in [2]. The enhancing is provided by the exponential decay of the amplitude for the wave-orbital motion: $a(z) = a(0) \exp(kz)$.

The analytically predicted dependences $B_v(a)$ and $B_v(u_*)$ can be verified empirically by estimating them in the tank experiments alike [27, 28]. The proper dependencies also could be estimated numerically by means of the direct numerical simulations alike [40] and using them for comparison with the presented analytical derivations (Eqs. 28, 29). Reliable results of these studies might open a way for numerous geophysical applications similar to ones followed the pioneer result [2].

Funding: This research was funded by the Russian Foundation for Basic Research, grant number 18-05-00161.

Acknowledgments: The author is grateful to Profs. V. Lykosov, N. Diansky, N. Huang, D. Dai, and Dr. A. Glazunov for their interest in the work and useful remarks. I am obliged to Prof. S. Longo for his kind permission to use the figures from his papers.

Conflicts of Interest: The authors declare no conflict of interest.

References

1. Polnikov, V.G. A Semi-Phenomenological Model for Wind-Drift Currents. *Boundary-Layer Meteorol*. **2019.** https://doi.org/10.1007/s10546-019-00456-1.
2. Qiao, F.; Yuan, Y.; Yang, Y.; Zheng, Q.; Xia, C.; Ma, J.: Wave-induced mixing in the upper ocean: Distribution and application to a global ocean circulation model. *Geophys. Res. Lett.* **2004**, *31*, L11303. doi:10.1029/2004GL019824.
3. Phillips O. M. A note of the turbulence generated by the gravity waves. *J. Geophys. Res*. **1961**, *66*, 2889-2893.
4. Stewart, R.W.; Grant, H.L. Determination of the rate of dissipation of turbulent energy near the sea surface in the presence of waves. *J. Geophys. Res*. **1962**, *67*, 3177-3180.
5. Kitaigorodskii, S. A.; Donelan, M.A.; Lumley, J. L.; Terrey, E.A. Wave-Turbulence Interactions in the Upper Ocean. Pt.II. Statistical Characteristics of Wave and Turbulent components of the Random Velocity Field in the Marine Surface Layer. *J. Phys. Oceanogr*. **1983**, *13*, 1988-1999.

6. Craig, P. D.; Banner, M. L. Modelling Wave Enhanced Turbulence in the Ocean Surface Layer. *J. Phys. Oceanogr*. **1994**, *24*, 2547-2559.
7. Kantha, L. H.; Clayson, C.A. An improved mixed layer model for geophysical applications. *J. Geophys. Res.* **1994**, *99*, 25,235–25,266 .
8. Ezer, T. On the seasonal mixed layer simulated by a basin-scale ocean model and the Mellor-Yamada turbulence scheme. *J. Geophys. Res*. **2000**, *105*, 16,843–16,855.
9. Teixeira, M.A.C.; Belcher, S.E. On the distortion of turbulence by a progressive surface wave. *J. Fluid Mech.* **2002**, *458*, 229-267.
10. Mellor, G.L. The three-dimensional current and wave equations. *J. Phys. Oceanogr*. **2003**, *33*, 1978–1989.
11. Polton, J. A.; Lewis, D.M.; Belcher, S.E. The role of wave-induced Coriolis-Stokes forcing on the wind-driven mixed layer. *J. Phys. Oceanogr*. **2005**, *35*, 444-457.
12. Phillips, O. M. *The dynamics of the upper ocean*. 2^{nd} ed. Cambridge Univ. Press, UK, 1977, 320 p.
13. Qiao, F.; Yuan, Y.; Ezer, T.; Xia, C.; Yang, Y.; Lü, X.; Song, Z.. A three-dimensional surface wave-ocean circulation coupled model and its initial testing. *Ocean Dynamics*. **2010**, *60*, 1339–1355 .
14. Belcher, S. E., Grant, A.L.M.; Hanley, K.E.; et al.(15 authors). A global perspective on Langmuir turbulence in the ocean surface boundary layer. *Geophys. Res. Lett*. **2012**, 39, L18605. doi:10.1029/2012GL052932.
15. Janssen, P.E.A.M. Ocean wave effects on the daily cycle in SST. *J. Geophys. Res*. **2012**, *117*, C00J32. doi:10.1029/2012JC007943.
16. Qiao, F.; Yuan, Y.; Deng, J.; Dai, D.; Song, Z. Wave–turbulence interaction-induced vertical mixing and its effects in ocean and climate models. *Phil. Trans. R. Soc*. **2016**, *A374*, 20150201. http://dx.doi.org/10.1098/rsta.2015.0201.
17. Walsh, K.; Govekar, P.; Babanin, A.V.; Ghantous, M.; Spence, P.; Scoccimarro, F. The effect on simulated ocean climate of a parameterization of unbroken wave-induced mixing incorporated into the k-epsilon mixing scheme, *J. Adv. Model. Earth Syst*. **2017**, *9*, 735–758, doi:10.1002/2016MS000707.
18. Mellor, G.L.; Yamada, T. Development of a turbulence closure model for geophysical fluid problems. *Rev. Geophys. Space Phys*. **1982**, *20*, 851–875.
19. Anis, A,; Moum, J.N.: Surface wave–turbulence interactions: Scaling $\varepsilon(z)$ near the sea surface. *J. Phys. Oceanogr*. **1995**, *25*, 2025–2045.
20. Li, Q.; Webb, A.; Fox-Kemper, B.; Craig, A.; Danabasoglu, G.; Large, W.G.; Vertenstein, M. Langmuir mixing effects on global climate: WAVEWATCHIII in CESM. *Ocean Modelling*. **2016**, *103*, 145-160. https://doi.org/10.1016/j.ocemod.2015.07.020.
21. Langmuir, I. Surface motion of water induced by wind. *Science*. **1938**, *38*, 119–123.
22. Craik, A.D.; Leibovich, S. A rational model for Langmuir circulations. *J. Fluid Mech*. **1976**, *73*, 401-426.
23. McWilliams, J.C.; Sullivan, P.P.; Moeng, C.-H. Langmuir turbulence in the ocean. *J. Fluid Mech*. **1997**, *334*, 1-30.
24. Lumley, J.L.; Terrey, E.A. Kinematics of Turbulence Convected by a Radom Wave Field. *J. Phys. Oceanogr.* **1983**, *13*, 2000-2007.
25. Babanin, A.V.: On a wave-induced turbulence and a wave-mixed upper ocean layer. *Geophys. Res. Lett.* **2006**, *33*, L20605 . http://dx.doi.org/10.1029/2006GL027308.
26. Benilov, A.Y. On the turbulence generated by the potential surface waves. *J. Geophys. Res.* **2012**, *117*, C00J30. doi:10.1029/2012JC007948.
27. Babanin, A.V.; Haus, B.K. On the existence of water turbulence induced by non-breaking surface waves. *J. Phys. Oceanogr*. **2009**, *39*, 2675–2679. doi:10.1175/2009JPO4202.1.

28. Dai, D.; Qiao, F.; Sulisz, W.; Han, L.; Babanin, A. An Experiment on the Nonbreaking Surface-Wave-Induced Vertical Mixing. *J. Phys. Oceanogr.* **2010**, *40*, 2180-2188 .
29. Terray, E. A.; Donelan, M. A.; Agrawal, Y. C.; Drennan, W.M.; Kahma, K. K.; Williams III, A. J.; Hwang, P. A.; Kitaigorodskii, S. A. Estimates of kinetic energy dissipation under breaking waves. *J. Phys. Oceanogr*. **1996**, 26, 792-807.
30. Gemmrich, J.R. Strong turbulence in the wave-crest region. *J. Phys. Oceanogr*. **2010**, *40*, 583–595. doi:10.1175/2009JPO4179.1.
31. Monin, A.S.; Yaglom, A.M. *Statistical Fluid Mechanics: Mechanics of Turbulence. V.1*. The MIT Press, Cambridge , 1971, 769 p.
32. Komen, G.; Cavaleri, L.; Donelan, M.; Hasselmann, K.; Hasselmann, S.; Janssen, P.A.E.M. *Dynamics and Modelling of Ocean Waves*. Cambridge University Press, UK, 1994, 544p.
33. Wu, J. Sea-surface drift currents induced by wind and waves. *J. Phys. Oceanogr*. **1983,** *13*, 1441-1451.
34. Yuan, Y.; Qiao, F.; Yin, X.; Han, L. Analytical estimation of mixing coefficient induced by surface wave-generated turbulence based on the equilibrium solution of the second-order turbulence closure model. *Science China: Earth Sciences*. **2013**, *56*, 71–80. doi: 10.1007/s11430-012-4517-x.
35. Polnikov, V.G. Features of air flow in the trough-crest zone of wind waves. **2010**. https://arxiv.org/abs/1006.3621.
36. Chalikov, D.; Rainchik, S. Coupled numerical modelling of wind and waves and theory of the wave boundary layer. *Boundary-Layer Meteorol*. **2011**, *138*, 1–41. doi:10.1007/s10546-010-9543-7.
37. Longo, S.; Chiapponi, L.; Clavero, M.; Mäkelä, T.; Liang, D. Study of the turbulence in the air-side and the water-side boundary layers in experimental laboratory wind induced surface waves. *Coastal Engineering*. **2012**, *69*, 67-81. doi:10.1016/j.coastaleng.2012.05.012.
38. Longo, S.; Liang, D.; Chiapponi, L.; Jimenez, L.A. Turbulent flow structure in the experimental laboratory wind-generated gravity waves. *Coastal Engineering*. **2012**, *64*, 1-15. doi:10.1016/j.coastaleng.2012.02.006
39. Babanin, A.V.; Chalikov, D. Numerical investigation of turbulence generation in non-breaking potential waves. *J. Geophys. Res*. **2012**, *117*, C00J17. doi:10.1029/2012JC007929.
40. Richter, D.H.; Sullivan, P.P. Momentum transfer in a turbulent, particle-laden Couette flow. *Physics of Fluids*. **2013**, *25*, 053304 . http://dx.doi.org/10.1063/1.4804391.